Polyelectrolytes tethered to a similarly charged surface

O. V. Borisov[a)]
LRMP/UMR 5067, 2, avenue du President Angot, 64053 Pau, France and Institute of Macromolecular Compounds of the Russian Academy of Sciences, 199004, St. Petersburg, Russia

F. A. M. Leermakers and G. J. Fleer
Wageningen University, Laboratory of Physical Chemistry and Colloid Science, Dreijenplein 6, 6703 HB Wageningen, The Netherlands

E. B. Zhulina
Institute of Macromolecular Compounds of the Russian Academy of Sciences, 199004, St. Petersburg, Russia and The University of Texas at Austin, Department of Chemistry and Biochemistry and Center for Polymer Research, Austin, Texas 78712

(Received 14 December 2000; accepted 9 February 2001)

Conformations of weakly charged quenched polyelectrolyte chains tethered to a similarly charged planar surface are analyzed on the basis of a combination of scaling, analytical, and numerical self-consistent field (SCF) approaches. Scaling theory predicts universal power law dependences of the large-scale conformational properties (like the end-to-end distance) of grafted chains on the overall surface charge per unit area. The SCF approach allows analysis of the detailed conformational structure of grafted polyions as a function of the distribution of immobilized charges between the surface and grafted chains. The analytical solution is only available in the limiting cases of sparse grafting of polyions to the charged plane and sufficiently dense grafting of polyions to a neutral surface. In the intermediate case when both interchain interactions and interaction of grafted chains with the surface are important, only numerical solutions can be obtained. We consider various ways to distribute the charges between the surface and the brush chains while keeping the sum of the two contributions constant. Upon increasing the charge on the surface, by concomitant reduction of the grafting density of the tethered chains we found: (i) an increase in height of the polymer layer; (ii) the development of a depletion zone of end points near the surface; and (iii) a sharpening of the end-point distribution with the peak shifting away from the surface. In the appropriate limiting cases excellent agreement of analytical SCF predictions is obtained with the numerical results. [DOI: 10.1063/1.1360244]

I. INTRODUCTION

Conformations of long, flexible charged polymer chains terminally attached to solid–liquid interfaces and forming so-called polyelectrolyte brushes have been extensively studied theoretically during the last decade[1–16] on the basis of scaling, analytical, and numerical SCF approaches. The combination of these theoretical methods has revealed both large-scale and local conformational properties of chains in polyelectrolyte brushes grafted to electrically neutral (uncharged) interfaces as a function of the main molecular parameters: (i) the number of monomers and the degree of ionization of the grafted chains and (ii) the density of grafting (the surface area per grafted chain). Some recent experimental observations[17–21] are in good agreement with the basic theoretical predictions, although systematic experimental studies of the intrinsic structure of grafted polyelectrolyte layers remain of considerable interest. The understanding of the conformations of grafted polyelectrolytes is relevant for a wide range of practical applications such as steric stabilization of colloidal dispersions in aqeuous media[22] and biological systems such as casein micelles,[23] exterior cell walls, etc.

Important features of polyelectrolyte brushes are the result of Coulombic interactions between charged monomers of the chains. These interactions are partially screened even in salt-free solution due to the presense of mobile counterions ensuring the electroneutrality of the system. In addition, in salt-added solutions the co- and counterions of the salt contribute significantly to this screening as well.

Up to now, the interactions of grafted polyions with the grafting surface are restricted to the impermeability of the half-space behind the surface for monomers of grafted chains and mobile ions. This condition of impermeability of the grafting surface for monomers and ions corresponds to the presence of a strong short-range repulsive potential which does not affect the conformations of grafted polyions on a large scale, especially when they are extended perpendicularly to the surface due to Coulombic interactions. However, the interaction of monomers with the grafting plane becomes important and may dramatically affect the structure of the polymeric layer when the surface itself is electrically charged.

The presence of immobilized charges on the surface results in long-range attraction or repulsion between the surface and the grafted chains. The effect of Coulombic attraction between grafted polyelectrolytes and an oppositely

a)Electronic mail: borisov@univ-pau.fr

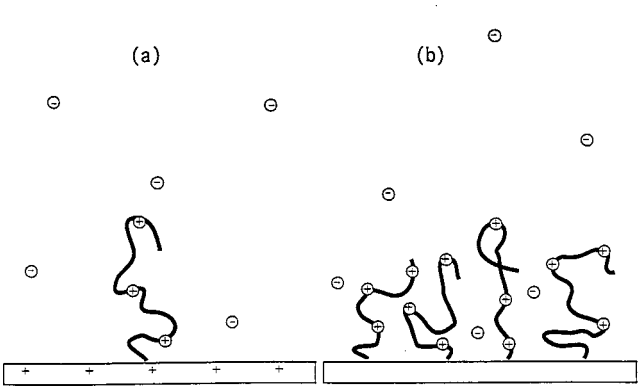

FIG. 1. A layer of polyelectrolyte chains grafted to the planar surface at low grafting density (individual chains or ''mushrooms'') (a) and at high grafting density (the ''brush'') (b).

charged surface has been recently studied in Refs. 24 and 25. In the present paper we focus on the case when the surface carries charged groups of the same sign as charged monomers in grafted chains. Indeed, these charged groups on the surface are often present in experimental systems because of dissociation of functional groups on the surface (e.g., for silica) or due to the adsorption of ionic surfactants on hydrophobic interfaces. Repulsion of charged monomers both from the charged interface and from monomers of other chains results in the extension of grafted polyions in the direction perpendicular to the surface. As we demonstrate below, the relative importance of these two repulsive forces determines the intrinsic conformational structure of the polyelectrolyte brush.

Up to now, the analysis of the Coulombic repulsion between charged monomers of a grafted chain and the grafting surface has been performed only for a single grafted polyelectrolyte chain.[26] This corresponds to the limit of infinite separation between the grafted polyions, where the interchain interactions do not play any role.

The aim of the present paper is to consider the influence of the surface charge on the conformations of grafted polyions in the brush regime, where both interchain repulsive interactions and long-range interaction of charged monomers with the charged surface are important.

This paper is organized as follows. In Sec. II we define the system and in Secs. III and IV we present scaling and SCF analytical results for two limiting cases: (i) sparse grafting to the charged surface (Sec. III) and (ii) dense grafting (brush regime) to a neutral surface (Sec. IV). The interplay between the effect of surface charges and the interchain Coulombic interactions is analyzed in scaling terms in Sec. V. Section VI includes results of numerical calculations, based on the Scheutjens–Fleer approach. Finally, in Sec. VII we summarize our conclusions.

II. MODEL AND PRELIMINARY CONSIDERATIONS

We consider a monolayer formed by long, weakly charged polyelectrolyte chains grafted at one end with a grafting density $1/s$ (s is grafting area per chain) onto an impermeable planar surface immersed in a solution, as sketched in Fig. 1. The grafting density is varied in a wide range including both the limit of individual noninteracting grafted chains at $1/s \cong 0$ [Fig. 1(a)] and the case of a dense polyelectrolyte brush consisting of strongly overlapping interacting polyions at $1/s \gg N^{-1}$ [Fig. 1(b)].

Let N be the degree of polymerization of grafted chains and α the fraction charged monomers; for convenience, we take this charge positive (i.e., polycations). The inverse value $m=\alpha^{-1}$ gives the number of neutral (uncharged) monomers in the chain between two neighboring charged ones. We assume α to be small (so that locally the chain obeys Gaussian statistics) and to be constant (quenched polyelectrolyte). The total charge on one polyion is $eQ=eN/m$, where $Q=\alpha N$ is the number of charges per chain.

We assume that the chains are flexible, i.e., the Kuhn segment length and the Bjerrum length $l_B=e^2/k_BT\epsilon$ (where ϵ is the dielectric permittivity of the solvent) are of the order of the monomer unit length a.

The grafting surface itself may be charged positively as well. We assume that the surface charge is uniformly distributed with a density $e\rho_s$ per unit area.

The overall charge immobilized per unit area of the surface includes both the contribution of the surface charge and that of grafted polyions: $e\rho=e\rho_s+e\rho_b$, where $\rho_b=Q/s$ is the brush charge.

The electroneutrality of the system as a whole is ensured by the presence of a compensating amount of mobile counterions in the solution. As the polyions are charged positively, the counterions are negative and taken to be monovalent.

An important length scale in the system is the Gouy–Chapmann length

$$\Lambda=(2\pi l_B\rho)^{-1}, \tag{1}$$

which characterizes the thickness of the counterion cloud above a homogeneously charged planar surface with an immobilized charge $e\rho$ per unit area in the absence of extra salt in the solution.[27]

We assume the excluded volume interactions between uncharged monomers to be weak, i.e., the solvent is a θ solvent for uncharged monomers. This assumption not only simplifies the analysis (the chains in the θ solvent obey Gaussian elasticity) but is also the relevant case for experimental systems. Many synthetic polyelectrolytes are only marginally soluble in water; the solubility is provided by the presence of charges in the chains while for uncharged monomers water is a rather poor solvent, i.e., the binary (excluded volume) interactions between uncharged monomers tend to be attractive. Typically the chains are extended due to electrostatic repulsion between the charges. On a small scale (of order of an elastic blob size[28]) the short-range attraction is not strong enough to induce the collapse of the chain, but it compensates the geometrical excluded volume effects such that the elastic response of the chain is like that of a Gaussian one. Under conditions of dense grafting (i.e., in the brush regime) the ternary interactions between uncharged monomers come into play and these induce additional swelling of the brush in a quasineutral regime.[5]

III. INDIVIDUAL POLYION GRAFTED TO A SIMILARLY CHARGED SURFACE

In the limit $Q/s \ll \rho_s$ the interaction between grafted polyions is negligible and their conformations are affected predominantly by the intramolecular Coulombic repulsion of the charged monomers and the repulsion from the similarly charged surface. Hence, we can use a single chain approximation and analyze the conformation of one grafted polyion subjected to the extensional electrostatic field created by the charged plane. Because of the condition $Q/s \ll \rho_s$ the Gouy–Chapmann length Λ in Eq. (1) is only determined by the surface charge $e\rho_s$; for this limit we use the symbol Λ_s.

The distribution of the dimensionless electrostatic potential, $\Psi(z) \equiv e\psi(z)/k_BT$, in the direction z perpendicular to a uniformly (positively) charged infinite planar surface and the density profile of the counterions, $c_i(z)$, in a salt-free solution can be obtained on the basis of the Poisson–Boltzmann equation[27]

$$\frac{d^2\Psi}{dz^2} = 4\pi l_B c_i(z), \tag{2}$$

$$c_i(z) = c_i(0)\exp(\Psi(z)), \tag{3}$$

with the boundary conditions $\Psi(0)=0$ and $(d\Psi(z)/dz)_{z=0} = -2/\Lambda_s$. The solution is given by

$$\Psi(z) = -2\ln(1+z/\Lambda_s), \tag{4}$$

$$c_i(z) = [2\pi l_B (z+\Lambda_s)^2]^{-1}, \tag{5}$$

where $\Lambda_s = (2\pi l_B \rho_s)^{-1}$ is the Gouy–Chapmann length, which characterizes the decay of the counterion density and can be interpreted as the characteristic thickness of the counterion cloud. It is noteworthy that the Debye screening length corresponding to the concentration of counterions at the distance Λ_s from the surface is of order of Λ_s. Hence, the Gouy–Chapmann length can also be interpreted as the electrostatic *screening length* in the cloud of counterions. Because of this screening the strength of the dimensionless electrostatic potential field decays with distance z from the plane as

$$-\frac{d\Psi}{dz} = \frac{2}{z+\Lambda_s}.$$

At distances $z \ll \Lambda_s$, this corresponds with a uniform electrostatic field, $4\pi l_B \rho_s$. For $z \gg \Lambda_s$ it decays as $\sim z^{-1}$. At such large distances $d\Psi/dz$ becomes independent of the surface charge density because of the screening of the surface charge by the cloud of counterions. Remarkably, the local screening length grows with the distance from the surface as $\sim z$.

The effect of the surface charge on the conformation of a grafted polyion has been analyzed in scaling terms in Ref. 26. The equilibrium extension of a grafted polyelectrolyte chain can be characterized by the average z projection, R_z, of the end-to-end vector **R**. The extension of the chain is determined by the competition between two forces: (i) the superposition of two extensional forces due to the intramolecular Coulomb repulsion, f_{intra}, and the repulsion f_s of the polyion by the similarly charged surface

$$f_{\text{intra}}/k_BT \cong l_B Q^2/R^2, \tag{6}$$

$$f_s/k_BT \cong -Q(d\Psi/dz)_{z\cong R_z}, \tag{7}$$

(ii) the elastic response arising in the extended chain because of conformational entropy losses

$$f_{\text{elastic}}(R_z)/k_BT \cong \frac{R_z}{Na^2}. \tag{8}$$

At zero surface charge the polyelectrolyte is extended only by intramolecular Coulomb repulsion and is characterized by its bulk dimension, $R_0 \cong Nam^{-2/3}(l_B/a)^{1/3}$. On a small scale the chain retains Gaussian statistics, while on a large scale it is fully extended and can be presented as a string of Gaussian electrostatic blobs of size $\xi_0 \cong m^{2/3}a(l_B/a)^{-1/3}$, each containing $g_0 \cong (\xi_0/a)^{1/2}$ monomers.[28–30]

At small surface charge, $f_s \ll f_{\text{intra}}$, the repulsion from the surface does not affect the extension of the grafted chain. Instead, it induces the orientation of the chain in the direction perpendicular to the surface. The onset of orientation can be determined from the condition $f_s R_0 \sim k_BT$, i.e., $\rho_{\text{orient}} \cong (QR_0 l_B)^{-1}$. At $\rho_s \ll \rho_{\text{orient}}$ the end-to-end vector of the chain has a random orientation in the hemisphere above the grafting surface. At $\rho_s \geqslant \rho_{\text{orient}}$ the mean-square fluctuation of the angle θ between the end-to-end vector and the direction normal to the surface scales as $<\theta^2> \cong \rho_{\text{orient}}/\rho_s$. Hence, the variation of the surface charge from 0 to $\rho_s \geqslant \rho_{\text{orient}}$ induces an increase in the *average* normal component of the chain dimension by the factor of $\pi/2$. This corresponds to the gradual transition from a random orientation of the end-to-end vector at $\rho_s = 0$ to strong orientation perpendiculary to the surface at $\rho_s \geqslant \rho_{\text{orient}}$.

The onset of an extra extension of the polyelectrolyte chain due to the repulsion from the surface corresponds to the condition $f_s \geqslant f_{\text{Coulomb}}$. This occurs at $\rho_s \geqslant \rho_{\text{ext}} \cong Q/R_0^2 \cong N^{-1}m^{1/3}(l_B/a)^{-2/3}a^{-2}$. At $\rho_s \geqslant \rho_{\text{ext}}$ the chain dimension in the z direction is determined by the force balance, $f_s \cong f_{\text{elastic}}$, and grows with increasing surface charge density ρ_s as

$$R_z(\rho_s) \cong \begin{cases} N^2 m^{-1}\rho_s l_B a, & \Lambda_s \geqslant Nm^{-1/2}a \\ Nm^{-1/2}a, & \Lambda_s \ll Nm^{-1/2}a. \end{cases} \tag{9}$$

At $\Lambda_s \geqslant Nm^{-1/2}a$ the screening length provided by the counterions cloud exceeds by far the z dimension of the chain. Then, the chain experiences an unscreened Coulombic repulsion from a uniformly charged surface. As a result the chain extension grows proportionally to the surface charge ρ_s. However, simultaneously with increasing $R_z(\rho_s)$ the Gouy–Chapmann length $\Lambda_s(\rho_s)$ decreases. Consequently, at large surface charge density, $\Lambda_s \ll R_z(\rho_s) \cong Nm^{-1/2}a$, the surface charge gets strongly screened from the polyion, and an additional increase in ρ_s does not affect the chain extension. The characteristic surface charge density corresponding to the screening of the surface charge from the polyion and to the leveling off of the $R_z(\rho_s)$ dependence, can be estimated from the condition $\Lambda_s(\rho_{\text{sat}}) \cong R_z(\rho_{\text{sat}})$ and scales as $\rho_{\text{sat}} \cong N^{-1}m^{1/2}a^{-1}l_B^{-1}$. Hence, the effect of the extra extension, as well as the width of the ρ_s range in which this extension occurs, increases with increasing m, i.e., is most pronounced for weakly charged polyelectrolytes.

The scaling arguments presented above give a qualitative picture of the influence of the surface charge on the extension of grafted polyions and explain the leveling off of the $R(\rho_s)$ dependence due to the effect of screening of the surface by counterions at large ρ_s.

We can get more detailed insight into the conformation of a polyelectrolyte chain grafted to a similarly charged surface using the strong stretching approximation similar to that suggested in Ref. 31.

In the strong stretching limit, $R_z \gg N^{1/2}a$, only the most probable (extended) conformations of the chain have to be taken into account, as these conformations give the major contribution to the partition function. This conformation can be characterized by the local extension, $E(z,R_z)=dz/dn$, which is a monotonous function of the z coordinate or of the monomer ranking number n ($n=0$ and $n=N$ correspond to the grafted and to the free end of the chain, respectively). We note that $3E(z,R_z)/2a^2$ is equal to the local tension in the chain at the distance z from the surface, while the inverse value, $c_p(z)=1/E(z,R_z)$ gives the monomer density profile in the z direction normalized to N (integrated over the area s per grafted chain). The free energy of the polyelectrolyte chain can be presented as a functional of the local extension and includes two terms describing the elastic free energy of an inhomogeneously extended Gaussian chain and the potential energy of charged monomers in the electrostatic field $\Psi(z)$ due to the charged plane. Hence,

$$F/k_BT=\frac{3}{2a^2}\int_0^{R_z}E(z,R_z)dz-m^{-1}\int_0^{R_z}\frac{\Psi(z)dz}{E(z,R_z)}, \quad (10)$$

where $\Psi(z)$ is given by Eq. (4).

Minimization of the free energy, Eq. (10) with respect to $E(z,R_z)$ and with respect to the z position of the chain end, R_z, under the constraint

$$\int_0^{R_z}\frac{dz}{E(z,R_z)}=N,$$

yields the distribution of the local extension in the chain,[32]

$$E(z,R_z)=\left[\frac{4}{3m}\ln\left(\frac{R_z+\Lambda_s}{z+\Lambda_s}\right)\right]^{1/2}a, \quad (11)$$

and of the average end position

$$(R_z+\Lambda_s)\mathrm{erf}\left(\sqrt{\ln\frac{R_z+\Lambda_s}{\Lambda_s}}\right)=\frac{2}{\sqrt{3\pi}}Nm^{-1/2}. \quad (12)$$

Here,

$$\mathrm{erf}(x)=\frac{2}{\sqrt{\pi}}\int_0^x\exp(-t^2)dt$$

is the error function.

Equation (12) for the average end position R_z can be also presented in reduced variables as

$$\sqrt{\frac{2}{\pi}}(h_g+\lambda_s)\mathrm{erf}\sqrt{\ln\frac{h_g+\lambda_s}{\lambda_s}}=1, \quad (13)$$

where we define the reduced Gouy–Chapmann length λ_s and the reduced average end-point coordinate h_g as

$$\lambda_s\equiv\Lambda_s/H_0, \quad h_g\equiv R_z/H_0.$$

The length H_0 is defined as

$$H_0=\sqrt{8/3\pi^2}Nm^{-1/2}a, \quad (14)$$

and coincides (with the accuracy of the numerical prefactor) with the maximal chain extension in the strong screening limit $\lambda_s \ll 1$.

Equations (12) and (13) give the *average* z position of the chain end in the extensional electrostatic field near a charged surface. We expect the fluctuations of the end position to be Gaussian with a characteristic width of order $\sim N^{1/2}a$.

It follows from Eq. (11) that the local chain extension decreases monotonically from the grafted end outwards and vanishes at the free end of the chain. According to Eq. (11) the monomer density $c_p(z)=1/E(z,R_z)$ increases monotonically with the distance z from the grafting plane. This reflects the decrease in the local tension in the chain.

In the asymptotic limits of weak and strong screening of the surface by counterions, we obtain from Eq. (12)

$$R_z(\rho_s)\cong\begin{cases}(2\pi/3)N^2\rho_s l_B m^{-1}a, & \Lambda_s \gg Nm^{-1/2}a\\ 2/\sqrt{3\pi}Nm^{-1/2}a, & \Lambda_s \ll Nm^{-1/2}a\end{cases} \quad (15)$$

or, in the reduced variables

$$h_g\cong\begin{cases}(\pi^2/8)\lambda_s^{-1}, & \lambda_s \gg 1\\ \sqrt{\pi/2}, & \lambda_s \ll 1.\end{cases} \quad (16)$$

In Eq. (15) we find the same exponents for the main variables as in Eq. (9). In contrast to the scaling result described by Eq. (9), Eq. (15) also gives the exact numerical prefactors.

Again, it follows from Eq. (15) or Eq. (16) that the overall chain stretching grows linearly with $\rho_s=(2\pi l_B\Lambda_s)^{-1}$ at small ρ_s and levels off at large ρ_s because of the screening effect of counterions. Using Eq. (11) we can compute the root-mean-square z position of the chain monomers, defined as

$$\langle z^2\rangle^{1/2}=\left(N^{-1}\int_0^{R_z}\frac{z^2dz}{E(z,R_z)}\right)^{1/2}.$$

We can express $\langle z^2\rangle^{1/2}$ in reduced variables by defining $\overline{h}\equiv\langle z^2\rangle^{1/2}/H_0$. From Eq. (11) we find

$$\overline{h}=\left(\frac{2}{\pi}\right)^{1/4}\left[\frac{1}{\sqrt{3}}(h_g+\lambda_s)^3\,\mathrm{erf}\sqrt{\ln\left(\frac{h_g+\lambda_s}{\lambda_s}\right)^3}\right.$$
$$-\sqrt{2}\lambda_s(h_g+\lambda_s)^2\,\mathrm{erf}\sqrt{\ln\left(\frac{h_g+\lambda_s}{\lambda_s}\right)^2}$$
$$\left.+\lambda_s^2(h_g+\lambda_s)\mathrm{erf}\sqrt{\ln\left(\frac{h_g+\lambda_s}{\lambda_s}\right)}\right]^{1/2}. \quad (17)$$

The asymptotic behavior of Eq. (17) is

$$\overline{h}\cong\begin{cases}(\pi^2/2\sqrt{30})\lambda_s^{-1}, & \lambda_s \gg 1\\ \sqrt{\pi/2\sqrt{3}}, & \lambda_s \ll 1.\end{cases} \quad (18)$$

The latter equation will be tested below using numerically exact computations.

IV. POLYELECTROLYTE BRUSH GRAFTED TO A NEUTRAL SURFACE

In this section we consider the opposite limiting case, $\rho_s \ll Q/s$, i.e., $\rho \cong Q/s$, when charged chains are grafted sufficiently dense to a weakly charged surface. In this case we can neglect the influence of the surface charge on the conformations of grafted polyions. The Gouy–Chapmann length is now determined by the brush charge only; for this limit we use the symbol Λ_b. The conformations are affected mostly by Coulombic interactions with other grafted chains and their counterions. The boxlike model of a polyelectrolyte brush grafted to a neutral surface has been studied in Refs. 1, 2, 5 on the basis of scaling arguments.

The essential feature of a polyelectrolyte brush is the extra extension of the grafted polyions in the z direction with respect to the dimension R_0 of a single polyion in the bulk of the solution due to interactions with other grafted chains and counterions. Two important length scales can be distinguished in the problem: the equilibrium brush thickness, $H \cong R_z$, and the bare Gouy–Chapmann length $\Lambda_b = (2\pi l_B \rho_s)^{-1}$, where $\rho_s = Q/e$. Depending on the ratio between H and Λ_b, two distinct regimes of behavior of polyelectrolyte brushes can be found.[1,5]

For relatively dense and strongly charged brushes, $\Lambda_b \ll H$, a so-called ''osmotic'' regime occurs. In this regime most of the mobile counterions are trapped inside the brush, compensating the immobilized charge of the tethered polyions. The brush is swollen due to the osmotic pressure of counterions. The balance between this osmotic pressure, $\Pi/k_BT \cong N/smH$, and the entropic elastic force given by Eq. (8) yields a scaling expression for the equilibrium thickness of the osmotic brush

$$H \cong Nm^{-1/2}a. \tag{19}$$

The essential feature of Eq. (19) is the independence of the brush thickness of the grafting density, s. Moreover, the exponents of the N- and m dependences in Eq. (19) coincide with those for a single chain grafted to a strongly charged surface in the limit of strong screening of the surface by counterions [second part of Eq. (15)]. In the brush case the limit $\Lambda_b \ll H$ corresponds to the strong screening of the Coulombic repulsion between the grafted chains by counterions trapped inside the brush. It is easy to prove[5] that, if $\Lambda_b \ll H$, the ''intrinsic'' Debye screening length κ_i^{-1}, provided by counterions localized inside the brush is much smaller than the overall brush thickness H. This implies that in the osmotic regime the brush is electroneutral locally on a scale larger than κ_i^{-1}. This provides the basis for the local electroneutrality approximation (LEA) widely used for the analysis of the intrinsic structure of osmotic brushes. Hence, the osmotic regime for the polyelectrolyte brush is analoguous to the regime of strong screening of the surface charge in the case of a single grafted polyelectrolyte chain.

At relatively sparse grafting of the polyions and low degrees of ionization, $\Lambda_b \gg H$, the electrostatic attraction between the grafted polyions and the mobile ions is not strong enough to trap the counterions inside the brush, and they spread in the half space above the surface within the characteristic length $\sim \Lambda_b$. The brush charge is not locally compensated, and the system can be envisioned as an electrical double layer formed by the brush and the (much thicker) cloud of counterions. The extensional force f_z applied to the grafted polyion can be estimated as the force of attraction between two oppositely charged layers and scales as $f_z/k_BT \cong l_B Q^2/s$. This force is balanced by the restoring elastic force arising in an extended chain, Eq. (8) resulting in the scaling dependence for the brush thickness

$$H \cong N^3 m^{-2} s^{-1} l_B a^2. \tag{20}$$

Comparison with Eq. (9) reveals that for the extension of a grafted polyion due to the repulsion from a charged surface in the weak screening limit, $\Lambda_b \gg Nm^{-1/2}a$, the scaling dependences in Eqs. (9) and (20) coincide if we write Eq. (9) as $H \cong N^2 m^{-1}\rho$ and set $\rho = \rho_s$ in the single chain case and $\rho = \rho_b$ (with $\rho_b = Q/s = s^{-1}N/m$) in the brush case.

Hence, in the scaling approximation, the conformation of weakly charged polyelectrolyte chains grafted to a planar surface depends only on the *overall surface charge* per unit area, ρ, regardless of the partitioning of this charge between grafted polyions and grafting surface.

However, a difference is expected on the level of the intrinsic structure (distribution of monomer units, counterions, free ends of grafted chains) which must be reflected in different numerical prefactors in the discussed asymptotic power dependences.

The intrinsic structure of polyelectrolyte brushes has been studied on the basis of LEA in Ref. 4 and in the opposite limit of weak screening in Ref. 15. The analytical solution without any preassumption about the counterions distribution interpolating between weakly charged and strongly charged (''osmotic'') regimes can be obtained[16] on the basis of the SCF approach developed earlier[31,33–35] for neutral brushes in combination with the PB equation for the electrostatic potential and counterion distribution. As has been shown in Refs. 31 and 33. the self-consistent potential experienced by a monomer unit in a monodisperse polymer brush formed by strongly extended Gaussian chains is of parabolic shape. This potential ensures strong fluctuations in the extension of chains in the brush, i.e., the free ends are distributed over the entire brush and the chains are extended inhomogeneously. The latter result is in pronounced contrast to the predictions of the boxlike model. The distribution $E(z',z)$ of local extension along the chain whose end is located at the distance z' from the surface is described[31] by the universal function $E(z,z') = (\pi/2N)\sqrt{z'^2 - z^2}$. In the case of a brush formed by polyelectrolyte chains all the excluded volume interactions in the brush can be neglected unless the grafting density is too large.[5] In this case the self-consistent potential per monomer coincides (with the accuracy of a factor m^{-1}) with the electrostatic potential, i.e.,

$$\Psi(z) = \text{const} - \frac{3\pi^2 z^2}{8a^2 N^2 \alpha} \equiv \text{const} - z^2/H_0^2, \tag{21}$$

where H_0 is still defined by Eq. (14) and scales as the thickness of the brush in the osmotic limit, Eq. (19), or as the

asymptotic extension of a single chain in the limit of strong screening of the surface charge, Eqs. (9) and (15) Thus, H_0 is an important universal length scale for the system of charged Gaussian chains tethered to a planar surface. The distribution of counterions inside the brush obeys the Boltzmann law

$$c_i(z)=c_i(0)\exp(-z^2/H_0^2), \tag{22}$$

while the distribution of charged monomer units $c_p(z)$ can be obtained by substitution of Eqs. (21) and (22) into the Poisson equation, which results in

$$c_p(z)/m=c_i(z)+(2\pi l_B H_0^2)^{-1}. \tag{23}$$

Hence, the density profiles of charged monomers and counterions inside the brush follow each other up to a constant difference: the density of uncompensated charges inside the brush is uniform throughout the brush and equal to $(2\pi l_B H_0^2)^{-1}$. The integral

$$\tilde{Q}=s\int_0^H [c_p(z)/m-c_i(z)]dz=\frac{sH}{2\pi l_B H_0^2}, \tag{24}$$

gives the value of uncompensated charge (per chain) inside the brush or, equivalently, the number of counterions leaving the brush. The overall height of the brush H (the cutoff length for the monomer density profile) and the unknown constant $c_i(0)$ are determined by the normalization condition

$$s\int_0^H c_p(z)dz=N,$$

and the condition of continuity of the electrostatic potential at the brush edge, i.e., at $z=H$. The electrostatic potential and the distribution of counterions at $z\geqslant H$ are described by Eqs. (4) and (5) with z substituted by $(z-H)$ and Λ_s substituted by $\tilde{\Lambda}_s=s/(2\pi l_B\tilde{Q})$; i.e., the outer edge of the brush plays the role of the charged surface with a charge per unit area $\tilde{Q}/s$, where $\tilde{Q}$ is again the uncompensated charge of the brush per chain.

Normalizing all the relevant length scales by H_0, we can introduce reduced variables

$$\lambda_b\equiv\Lambda_b/H_0, \quad h\equiv H/H_0, \quad \zeta\equiv z/H_0.$$

In these reduced variables the density profiles of monomers and counterions inside the brush read

$$c_p(\zeta)/m=c_0\lambda_b[1+h^2\exp(h^2-\zeta^2)], \tag{25}$$

$$c_i(\zeta)=c_0\lambda_b h^2\exp(h^2-\zeta^2), \tag{26}$$

where $c_0=Q/sH_0$, and the reduced overall brush thickness h is given by

$$h+\frac{\sqrt{\pi}}{2}h^2\exp(h^2)\mathrm{erf}(h)=\lambda_b^{-1}. \tag{27}$$

The fraction of uncompensated charge (the fraction of counterions leaving the brush and localized at $z>H$) is given by

$$\tilde{Q}/Q=\lambda_b h. \tag{28}$$

Using Eqs. (25) and (27), one can also obtain an equation for the reduced root-mean-square z position of the chain segments

$$\overline{h}=\sqrt{\tfrac{1}{2}[1-\lambda_b(h+h^3/3)]}. \tag{29}$$

The free-end distribution $g(z)$ can be obtained by inverting the equation for the monomer density

$$c_p(z)=\frac{1}{s}\int_z^H\frac{g(z')dz'}{E(z,z')}. \tag{30}$$

In the reduced variables, $g(\zeta)$ is given by

$$g(\zeta)=\lambda_b\zeta\left[\frac{1+h^2}{\sqrt{h^2-\zeta^2}}+\sqrt{\pi}h^2e^{h^2-\zeta^2}\,\mathrm{erf}(\sqrt{h^2-\zeta^2})\right]. \tag{31}$$

It follows from Eqs. (25)–(31) that all the properties of the polyelectrolyte brush are governed by the dimensionless parameter λ_b which describes the strength of attraction of counterions to the oppositely charged brush. The parameter λ_b decreases with increasing surface charge $\rho=Q/s$ and determines the degree of localization of counterions inside the brush [cf. Eq. (28)].

It is easy to prove that in accordance with the scaling prediction the limit $\lambda_b\ll 1$ corresponds to the localization of counterions inside the brush

$$\tilde{Q}/Q\cong\lambda_b\sqrt{\ln(2/\lambda_b\sqrt{\pi})},$$

while in the opposite limit $\lambda_b\gg 1$ counterions leave the brush. The brush charge remains uncompensated to the extent

$$\tilde{Q}/Q\cong(1-\lambda_b^{-2}).$$

The corresponding asymptotic limits for the reduced total and root-mean-square brush thickness are given by

$$h\cong\begin{cases}\lambda_b^{-1}, & \lambda_b\gg 1\\ \sqrt{\ln(2/\lambda_b\sqrt{\pi})}, & \lambda_b\ll 1\end{cases} \tag{32}$$

and

$$\overline{h}\cong\begin{cases}(\lambda_b\sqrt{3})^{-1}, & \lambda_b\gg 1\\ (\sqrt{2})^{-1}, & \lambda_b\ll 1.\end{cases} \tag{33}$$

The corresponding asymptotic distribution of the monomer density and of the free ends are given by

$$c_p(\zeta)/m\cong\begin{cases}\lambda_b c_0, & \lambda_b\gg 1\\ (2c_0/\sqrt{\pi})\exp(-\zeta^2), & \lambda_b\ll 1\end{cases} \tag{34}$$

$$g(\zeta)\cong\begin{cases}\dfrac{\zeta}{h}\dfrac{1}{\sqrt{h^2-\zeta^2}}, & \lambda_b\gg 1\\ \dfrac{2}{\sqrt{\pi}}\exp(-h^2)\dfrac{\zeta}{\sqrt{h^2-\zeta^2}}+2\zeta\exp(-\zeta^2), & \lambda_b\ll 1.\end{cases} \tag{35}$$

Equations (34) and (35) show that with increasing $\rho=Q/s$, i.e., with decreasing λ_b the average monomer density in the brush decreases (extension of chains) while the monomer density profile becomes smoother and changes from step-like at $\lambda_b\gg 1$ to a Gaussian shape at $\lambda_b\ll 1$. In the limit $\lambda_b\ll 1$ the density of the free ends $g(\zeta)$ monotonously increases with ζ and diverges at the outer brush edge, $\zeta=h$. This means that most of the chain ends are localized near the

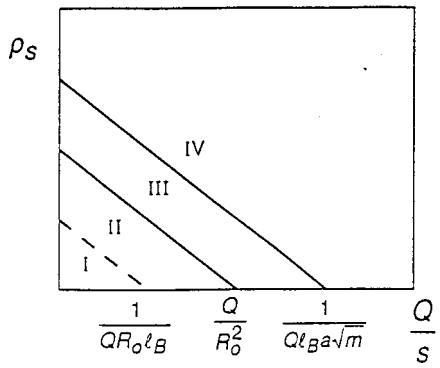

FIG. 2. The diagram of states of a grafted polyelectrolyte layer in the $(\rho_s, Q/s)$ plane. Explanation in the text.

brush edge (which is characteristic for a steplike monomer density profile, cf. Refs. 31, 34, 35). With decreasing λ_b, in addition to the edge maximum a second maximum in the central region (at $\zeta \cong 1/\sqrt{2}$) appears. This shows that the fluctuations of the chain extension throughout the brush increase.

The reduced average end position [the first moment of the distribution function of the free ends, Eq. (31)] is given by

$$h_g = \frac{\pi}{4}\lambda_b e^{h^2} h^2. \tag{36}$$

The corresponding asymptotics for h_g can be obtained by taking into account Eq. (27) to give

$$h_g \cong \begin{cases} (\pi/4)\lambda_b^{-1}, & \lambda_b \gg 1 \\ \sqrt{\pi}/2, & \lambda_b \ll 1. \end{cases} \tag{37}$$

V. POLYELECTROLYTE BRUSH GRAFTED TO A CHARGED SURFACE

The results of Secs. III and IV for a single polyion grafted to a charged plane and for a brush of charged chains grafted to a neutral surface show that the conformations of grafted chains depend on the density ρ of the charge immobilized per unit area of the surface in a similar way for the two cases. In the former limit ρ is mainly determined by the surface charge ρ_s, in the latter by the brush charge $\rho_b = Q/s$. At small charge density ρ the extension of grafted chains grows proportionally to ρ, whereas at large surface charge density the Coulombic repulsion gets strongly screened by counterions and the dependence of the chain extension on ρ levels off towards a characteristic value proportional to $Nm^{-1/2}a$. Hence, within the accuracy of the scaling approximation the conformations of polyions grafted to a charged surface depends only on the total value of charge immobilized per unit area, regardless of its partitioning between grafted polyelectrolytes and the grafting plane. This is reflected by the diagram of states in (ρ_s, ρ_b) coordinates presented in Fig. 2. Each cross section of the diagram parallel to one of the axes corresponds to an increase in one of the components (ρ_s or ρ_b) of the total charge per unit area ρ, while all other cross sections correspond to variations of both components. The regions of the diagram correspond to randomly (I) or strongly (II) oriented polyions of size R_0, to the regime of unscreened Coulomb repulsion (III) with growing extension, and to the regime of strongly screened Coulomb repulsion (IV). Within each region the chains extension obeys the particular scaling dependences on N, m, ρ. This means that, within the scaling approximation, the chain dimension remains constant along the cross section of the diagram with the slope equal to -1 (parallel to the boundaries between the regions of the diagram).

This universality breaks down for intrinsic structural properties of the layer, such as the monomer and the free-end densities, the local tension in grafted chains, etc. Also, the exact numerical prefactors or non-power-law dependences of the large scale (integral) properties (chain extension, average end position, etc.) on the main parameters (N, m, ρ) are different in the various regimes. The relative contributions of ρ_s and ρ_b must strongly affect all these properties. In other words, in addition to the universal scaling dependences of large-scale properties on the total surface charge density ρ there are also non-power-law dependences for each of them on the fraction β of the overall surface charge immobilized on the grafted chains

$$\beta = \rho_b/\rho,$$

or

$$\rho_b/\rho_s = \beta/(1-\beta).$$

The main tendency in the β dependences follows from the analysis of the asymptotic behavior of the monomer and the free-ends density profiles and their moments (the average root-mean-square monomer position and the average end positions) in the limiting cases $\beta = 0$, i.e., individual polyions grafted to a charged plane (Sec. III) and $\beta = 1$, i.e., a polyelectrolyte brush grafted to a neutral surface (Sec. IV).

The monomer density profile $\sim E^{-1}(z, R_z)$ in a single polyelectrolyte chain, given by Eq. (11) is a monotonically *increasing* function of z (which formally diverges at $z = R_z$), whereas the monomer density profile in the brush is, in contrast, a monotonically *decreasing* function of z, according to Eq. (25).

In the general case that the contribution to the overall surface charge density $\rho = \rho_s + \rho_b$ provided by the charges immobolized on tethered chains is comparable to that of the charges immobilized on the grafting plane, $\beta \sim (1-\beta)$, the analytical SCF approach combined with the PB equation fails to describe the brush structure. The system in this case is analogous to a polymer brush subjected to an external extensional force or a polymer brush grafted to a surface with positive curvature (convex surface). In these cases a ''dead zone'' appears near the surface where no free ends of the chains are found. In other words, switching on an external extensional field suppresses the *relative* fluctuations of the extension of grafted chains in the brush in comparison to the brush in which chains are extended only due to the self-consistent molecular potential. We have evidence for this behavior from the analysis of the two limiting cases.

(i) The magnitude of fluctuations of the chain extension in the brush grafted to a neutral surface scales as the brush thickness (or the average end position) regard-

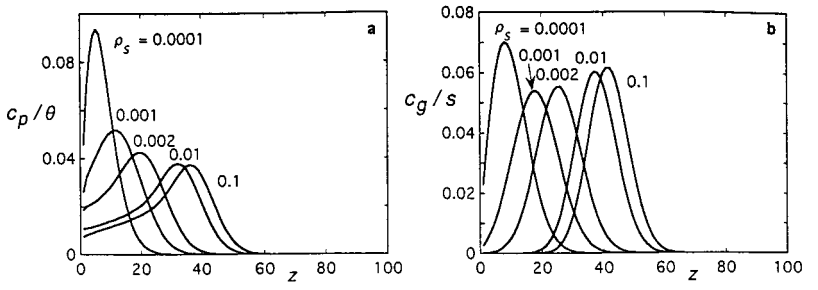

FIG. 3. The monomer density profiles (a) and the distribution of the chain end (b) for a single polyelectrolyte chain, $N=200$, $m=10$ for various surface charge densities ρ_s (shown at the corresponding curves). All profiles are normalized to unity.

less of the grafting density, i.e., the relative fluctuations remain of order of unity (the numerical factor of course changes with the brush structure as the grafting density increases).

(ii) In the opposite case of a single chain grafted to a charged surface, an increase in the surface charge results in an increase in the average chain extension, while the magnitude of fluctuations of this extension remains of order of the Gaussian chain size, $N^{1/2}a$. Hence, with increasing chain extension the relative magnitude of the fluctuations decreases and a wide dead zone (where the probability to find the chain end almost vanishes) is expected proximal to the surface.

VI. SCF RESULTS

To analyze the structure of a polyelectrolyte brush grafted to a charged plane in the general case, where brush and surface charges may be of comparable magnitude, we use the numerical SCF approach based on the Scheutjens–Fleer algorithm[36] adjusted to charged systems.[37] We have performed calculations for grafted chains consisting of $N=200$ or $N=100$ monomers for $m=10;5;2$ (i.e., for a fraction of charged monomers $\alpha=0.1;0.2;0.5$) and variable grafting density and surface charge density. The volume fraction of salt in the bulk of the solution was kept sufficiently low ($c_s=10^{-7}$) in order to ensure quasi-salt-free conditions for grafted polyelectrolytes. The system size was fixed to 500 lattice layers of characteristic length $a=0.3\,\mathrm{nm}$. The dielectric constant was fixed to $\epsilon=80$, which results in a Bjerrum length $l_B=2.4a$. A cubic lattice was used. The θ conditions with respect to interactions between uncharged monomers were used and there were no specific interactions between the monomers and the grafting surface.

A. Single chain grafted to a charged surface

Figure 3 shows the evolution of the overall monomer density profile $c_p(z)$ and of the distribution of the free end for an individual grafted polyion ($N=200$, $m=10$) with increasing surface charge density ρ_s. The grafting density is chosen equal to $1/s=\theta/N=0.5\cdot10^{-6}$ so that interaction of polyions is negligible; here, θ is the amount of polymer expressed in equivalent monolayers.

We first discuss the free ends [Fig. 3(b)]. As expected, the position of the maximum in the distribution of the free end (corresponding to R_z) is monotonically displaced towards larger z. This reflects the orientation and a growing extension of the polyion with increasing ρ_s. The extension is saturated, i.e., becomes virtually unaffected by ρ_s at $\rho_s \geqslant 10^{-2}$, which coincides with our estimation for $\rho_{\mathrm{sat}} \cong N^{-1}m^{1/2}a^{-1}l_B^{-1}$ at $N=200$, $m=10$. At the same time the end-point distribution retains a symmetrical (Gaussian) shape. The width of the distribution weakly decreases as the overall chain extension increases. When the chain is extended due to the repulsion from the charged grafting surface, a dead zone proximal to the surface appears, which grows as ρ_s increases. This reflects the independence of the fluctuations of the end position of the chain extended by an external (nonfluctuating) field.

The overall density profiles [Fig. 3(a)] also show the growing extension of the chain with increasing surface charge density ρ_s. With increasing ρ_s the monomer density profiles become more and more asymmetrical. In the range $0<z\leqslant R_z$ the density monotonically increases. This reflects the monotonic decrease in the local tension along the chain, cf. Eq. (11). Whereas Eq. (11) predicts formally a divergence of the monomer density at $z=R_z$, the calculated density profiles have a sharp maximum at $z\cong R_z$ which is followed by a steep decay resulting from Gaussian fluctuations occurring predominantly in the weakly extended outermost parts of the chain.

The extension of the chains as a function of the polyelectrolyte charge m^{-1} is plotted in Fig. 4, for a highly charged surface ($\rho_s \gg \rho_{\mathrm{sat}}$). In this graph the extension is characterized by several measures: the average z position and the root-mean-square position of the free end normalized to N, and the average position and the root-mean-square position of all the chain monomers. These dimensions are nor-

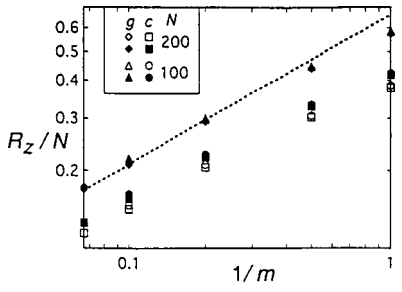

FIG. 4. The average position (open symbols) and the root-mean-square position (filled symbols) for both the end segment (diamonds, triangles) as well as for all the chain segments (squares, circles) of a single grafted polyelectrolyte as a function of the fraction of charged monomers m^{-1}, in double-logarithmic coordinates. The dashed line has a slope of 1/2. The results (normalized to N) are given for $N=100$ and $N=200$; the surface charge ρ_s is 0.1.

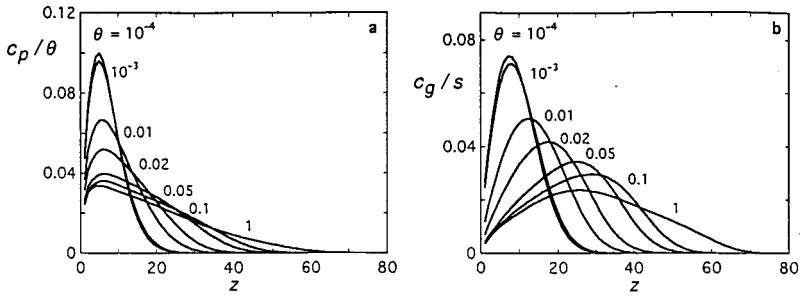

FIG. 5. The monomer density profiles (a) and the distribution of the chain end (b) for chains in a polyelectrolyte brush ($N=200$, $m=10$) grafted to a neutral surface, for various grafting densities. The profiles are normalized to unity. The grafting density $1/s$ equals θ/N; the values of θ are given in the plot.

malized to N and given for two chain lengths. In all cases the observed slope (in log–log coordinates) is close to 1/2, which is in line with the prediction given by Eq. (9).

B. Brush grafted to a neutral surface

Figure 5 presents the overall monomer density profiles and the free-end distribution in a polyelectrolyte brush grafted to a neutral planar surface. Again, both profiles are normalized to unity. The grafting density $1/s=\theta/N$ is varied in the range from $0.5\cdot 10^{-6}$ to $0.5\cdot 10^{-2}$ ($N=200$). With increasing grafting density the charge ρ_b per unit area of the surface increases proportionally. This gives rise to an orientation and an additional extension of the grafted polyions, as discussed in Sec. IV. The extension grows monotonically with ρ_s and levels off at large grafting density, just as in the case of a single chain grafted to a surface with increasing charge density ρ_s. However, the corresponding changes in the monomer density profile and in the free-end distribution are qualitatively different.

With increasing grafting density (accompanied by increasing extension of the chains) the monomer density profile is relatively flat and shows the Gaussian shape as predicted by Eq. (34) for the osmotic brush in the limit $\lambda_b \ll 1$, as seen in Fig. 5(a). With decreasing grafting density the brush becomes more compact and the decay of the monomer density near the brush edge becomes sharper. We note that Eq. (34), which does not take into account fluctuations of the chain extension on the scale $\leqslant N^{1/2}a$, predicts an abrupt drop in the monomer density at the brush edge, $z=H$. This jump is smeared out due to Gaussian fluctuations around the most probable (extended) conformation: the contribution of this fluctuation is most important in the terminal (unstretched) parts of the chains.

The evolution of the distribution of free ends, Fig. 5(b), with increasing density of grafting of polyelectrolyte chains occurs markedly different from the case of one grafted polyion [cf. Fig. 3(b)]. As the maximum of the distribution gets displaced to larger values of z, reflecting the higher chain extension, the distribution itself becomes broader and the value at the maximum progressively decreases. Clearly there are strong fluctuations of the extension of chains in the parabolic self-consistent electrostatic field in the polyelectrolyte brush. The magnitude of these fluctuations scales as $\sim Na$ and the free ends of the chains are distributed throughout the brush. The distribution of free ends in a free (unconfined) polyelectrolyte brush is found to be unimodal in the whole range of grafting densities. Hence, the formal divergence at the edge maximum as predicted by Eqs. (31) and (35), based on the strong stretching approximation, is smeared out [just like the jump in the monomer density profile at $z=H$ according to Eq. (34)], due to the same Gaussian fluctuations of terminal (nonstretched) parts of the chains that reach the brush edge.[38]

Figure 6 gives the proof of the $H\sim m^{-1/2}$ dependence of the polyelectrolyte brush thickness in the limit of large grafting density; this dependence was predicted in Eq. (19). As in Fig. 4 both the first moment and the second moment of the distribution of the end point as well as the overall density profile are given for two chain lengths $N=100,200$. The dotted line in Fig. 6 is the predicted scaling dependence and it is clear that the numerical results are in good agreement with the analytical predictions.

C. Polyelectrolyte brush grafted to a charged surface

As discussed in Sec. V, the partitioning of the overall charge ρ between the grafting surface and the grafted chains does not affect the scaling (power-law) dependences of the large-scale properties of the chains on the overall charge. This is reflected by the diagram of states, shown in Fig. 2. However, we expect weaker (non-power-law) dependences of the large-scale properties on the partition coefficient $\beta=\rho_b/\rho$. As a result, the distribution of the electrostatic potential and of the intrinsic brush structure (monomer and free-ends density profiles) is affected by the partition of the immobilized charge between the chains and the surface. We have seen an indication of this in the qualitatively different

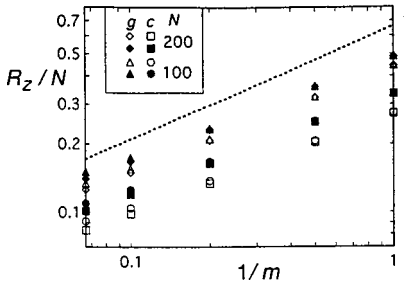

FIG. 6. The average position (open symbols) and the root-mean-square position (filled symbols) for both the end segment (diamonds, triangles) as well as for all the chain segments (squares, circles) of a polyelectrolyte brush grafted to a neutral surface as a function of the fraction of charged monomers m^{-1}, in double-logarithmic coordinates. The dashed line shows the slope 1/2. The results (normalized to N) are given for $N=100$, $N=200$; the grafted amount $\theta(\equiv N/s)$ equals 5 monolayers.

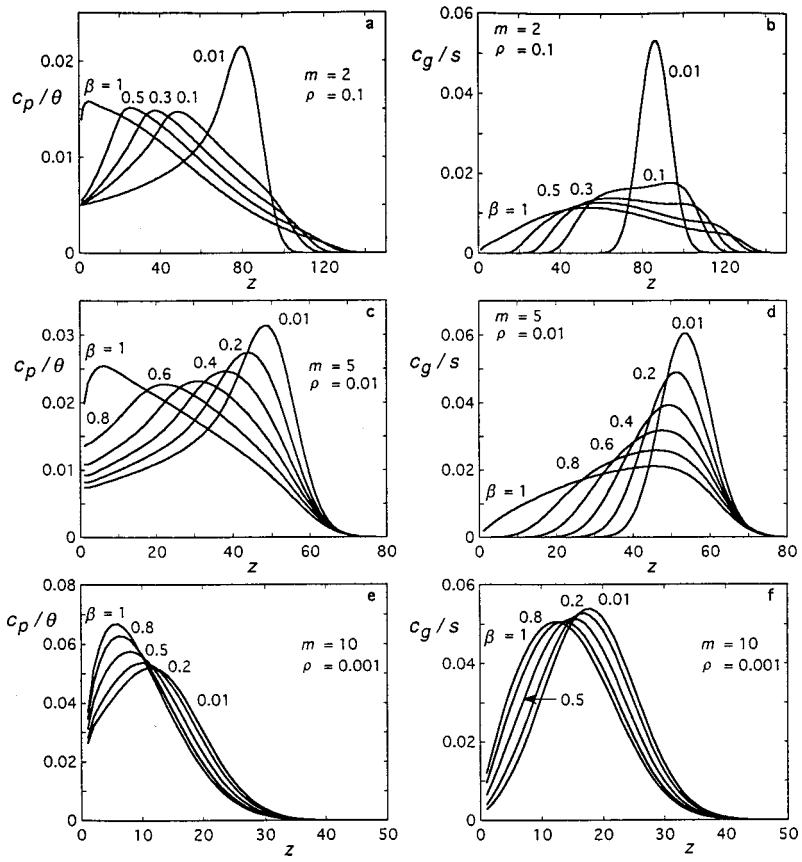

FIG. 7. Normalized monomer density profiles (a, c, e) and normalized density profiles for the chain end (b, d, f) for chains in a polyelectrolyte brush grafted to a charged surface, at constant value of the overall surface charge $\rho=0.1$ (a,b), 0.01 (c,d) and 0.001 (e,f). $N=200$, $m=2$ (a,b),5 (c,d),10 (e,f), values of β as indicated. A decrease of β (i.e., a higher relative contribution of the surface charge) is accomplished by decreasing the grafting density $1/s$.

density profiles obtained both analytically and numerically for the cases $\beta=0$ (single chain at charged surface) and $\beta=1$ (polyelectrolyte brush grafted to neutral surface).

Figure 7 illustrates the evolution of the overall monomer density profile (left) and of the distribution of free ends (right) for various values of the partition coefficient β, at three constant overall charge densities $\rho=\rho_s+\rho_b$, namely $\rho=10^{-1}$, 10^{-2}, and 10^{-3} and for three typical cases of $m=2,5,10$. As before, the profiles are normalized to unity. The highest value $\rho=10^{-1}$ corresponds to the regime of strong screening, $\lambda\ll 1$, the lowest ($\rho=10^{-3}$) to a considerable fraction of counterions escaping the brush ($\lambda\gg 1$).

The monomer density profiles in Fig. 7(a), at $\beta\approx 1$ are close to the Gaussian one found for the polyelectrolyte brush grafted to neutral surface [compare Eq. (34) and Fig. 5(a)]. The maximum of the distribution is localized near the surface and the monomer density decays continuously with increasing distance from the surface (except for a small proximal region where purely steric restrictions result in some depletion). With decreasing β (increasing charge on the surface and simultaneous decrease in the number of grafted chains per unit area), the maximum of the monomer density gets displaced towards the periphery of the brush, and at $\beta\ll 1$ the monomer density becomes an increasing function of z throughout the brush, except for the edge region, $z\cong H$; the maximum density is now localized near the brush edge.

The distribution of free ends in the polyelectrolyte brush is even more sensitive to the surface charge. Figure 7(b) shows that even at a small surface charge the proximal dead zone, i.e., a region without free ends, appears. This is expected because the effect of the similarly charged grafting surface is equivalent to that of an external extensional force field. With increasing surface charge ρ_s (at given total charge $\rho=0.1$) the dead zone becomes progressively wider, while the width of the maximum of the distribution becomes smaller and the maximum gets sharper. Hence, the surface charge pushes the ends away from the surface and simultaneously suppresses the fluctuations of the end position. The end-point distribution becomes more or less bimodal in the intermediate range of $\beta\approx 0.5$.

We conclude that the intrinsic structure of the polyelectrolyte brush is strongly affected by the fraction of charge immobilized on the grafting surface. Also, it follows from Figs. 7(a) and 7(b) that a decrease in β (repartitioning of charge towards the surface) results in a weak decrease in the overall chain extension. This effect cannot be predicted on the basis of a scaling analysis.

With decreasing ρ (downward in Fig. 7) the pronounced effect of the partitioning coefficient β is gradually lost. Especially in the bottom diagrams ($\rho=10^{-3}$), the degree of charge is too small to induce strong stretching. In this case the variation of β does not lead to a siginifcant variation in the density profiles.

The effect of the partitioning of the charge β on the thickness of the brush, characterized by the root-mean-square monomer position $\overline{h}$ (left) and average end position h_g (right) is illustrated in Fig. 8. In these diagrams, $\overline{h}$ and h_g are plotted as a function of β at constant overall charge. Analytical predictions for $\overline{h}$ and h_g are only available for $\beta=0$ and

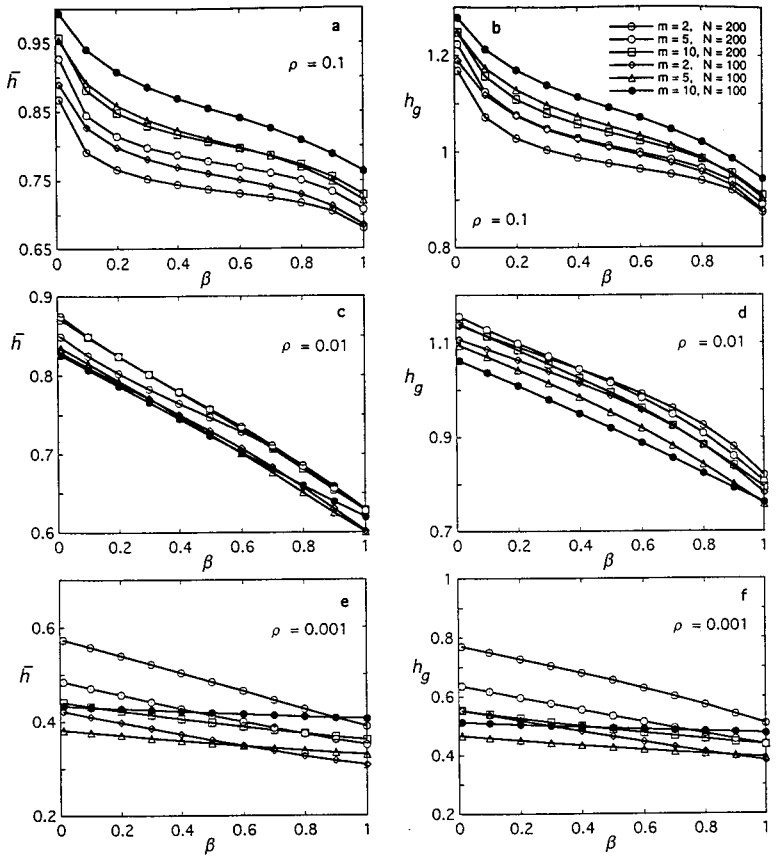

FIG. 8. The reduced root-mean-square position of the chain monomers (left) and the reduced average end position (right) in a polyelectrolyte brush grafted to a charged surface as a function of the relative charge $\beta = \rho_b/\rho$ immobilized on the grafted chains, for two chain lengths ($N=100$ and 200) and three brush charge densities. The symbols, as illustrated in diagram b, apply for all diagrams. The total charge in the system is $\rho=0.1$ (top diagrams), 0.01 (middle), and 0.001 (bottom).

$\beta=1$. The numerical SCF theory can also provide the intermediate cases. It follows from Fig. 8 that, at given overall charge (given λ) the average end position and the average monomer position (the thickness of the brush) decrease with increasing β. For low values of ρ (10^{-2} and 10^{3}), the intermediate situations may be approximated as a linear interpolation between $\beta=0$ and $\beta=1$. However, at high values of the overall surface charge the interpolation between the two analytical limits is not a straight line. The dependence of the average height of the brush layer on the charge partitioning is then rather weak at intermediate values of β and it is stronger for high and low values of β. The variations shown in Fig. 8 lead to some interesting phenomena, as will be shown in the next figure.

An alternative presentation of the numerical results is to give the thickness of the polymer layer as a function of the overall charge in the system. In these coordinates the analytical predictions can be compared more easily with the numerical data. Therefore, we present in Fig. 9 the root-mean-square monomer position $\bar{h}$ and average end position h_g as a function of the inverse reduced overall charge per unit area λ for three values of the partition coefficient: $\beta=1$, 0.5, and 0.01. Dashed lines correspond to analytical results for $\beta=0$, according to Eqs. (17) and (13) In this case $\rho=\rho_s$ and essentially all the charge is localized on the grafting surface. The dotted lines correspond to analytical results for the case of polyelectrolyte brush grafted to a neutral surface ($\beta=1$), where all the charge is localized on the grafted chains: $\rho=\rho_b$. For this situation we have Eqs. (29) and (36) for the average monomer position and the average end position, respectively. The results of Fig. 9 indicate that the numerical data nicely approach the analytical predictions both for the average end point and for the overall average monomer position of the chains. This follows from:

(i) in panels a and b the points which present systems with $N=100$, 200 and $m=2$, 5, 10 all collapse onto the predicted dotted line for $\beta=1$;

(ii) as shown in panels e and f, the numerical data collapse onto the predicted dashed line applicable for very low values of β. The correspondence with the average end position is slightly better than with the average overall density.

At intermediate values of β the numerical data points show an interesting behavior. Close inspection indicates that near $\lambda=0.1$ there is a weak local maximum in the overall height of the brush as well as in the average height of the end points. This maximum is generated because at intermediate values of β the end-point position tends to remain close to the dashed line for large values of λ, whereas it remains near the dotted line for small values of λ. When λ is large there are only a few charges in the system, and varying this distribution over surface and brush will not result in a lot of stretching. That is why the influence of β is not very strong in this part of the plot. On the other hand, when λ is small there are many charges. When this charge is mostly on the chains ($\beta=1$), the brush is in the osmotic regime. Distributing the charge gradually to the surface has initially only a minor effect because the charge on the surface is screened by

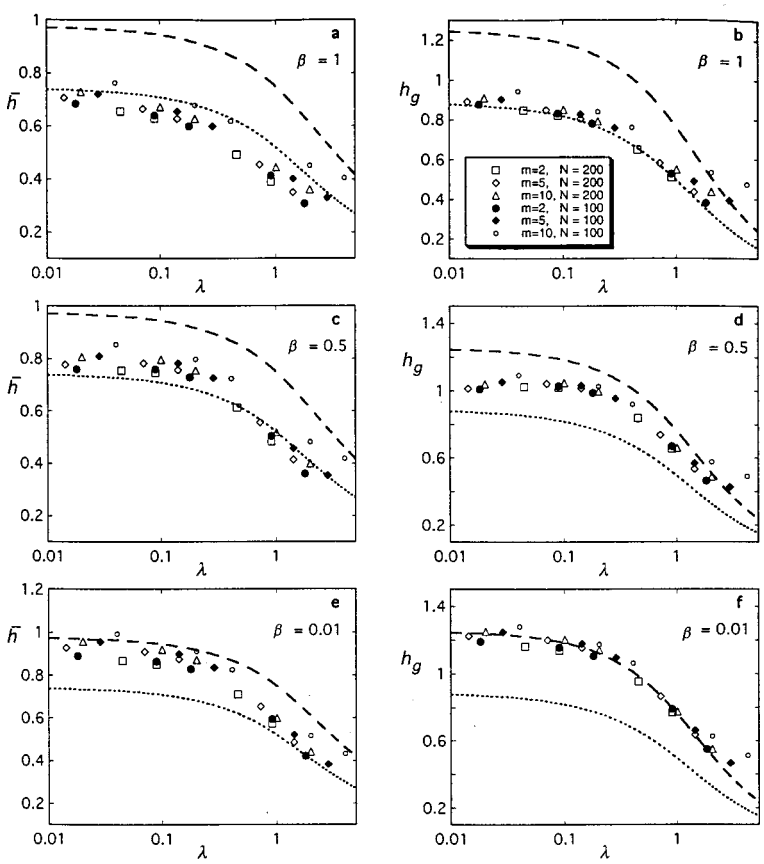

FIG. 9. The reduced root-mean-square position of the chain monomers (left) and the reduced average end position (right) in a polyelectrolyte brush grafted to a charged surface as functions of the reduced charge per unit area λ for various values of $\beta=1$ (top diagrams), 0.5 (middle), 0.01 (bottom). Data for $N=200$, $m=10,5,2$, $N=100$, $m=10,5,2$ are given and the symbols, as illustrated in diagram b, apply for all diagrams. The dashed lines give $\bar{h}$ (left) and h_g (right) as predicted by Eqs. (17) and (13) for individual chain grafted to charged surface, $\beta=0$, and the dotted lines correspond to the analytical prediction for $\bar{h}$ (left) Eq. (29) and h_g (right) Eq. (36) for a polyelectrolyte brush grafted to a neutral surface, $\beta=1$.

the ions in the brush. For intermediate β values the brush remains in the osmotic regime (when λ is small) and the numerical points are found near the dotted line. At intermediate values of λ the osmotic regime is easily lost and the numerical points move towards the dashed line.

VII. CONCLUSIONS

Both a scaling and an SCF analysis of polyelectrolyte chains grafted to the similarly charged surface show that the main quantity which determines these conformations is the overall charge ρ immobilized per unit area of the interface. This overall charge is the sum of the contributions ρ_s from the charge on the surface and the charge ρ_b on the grafted chains. In the framework of the scaling approximation (within the accuracy of asymptotic power dependences), the average extension of chains depends *only* on the overall charge ρ per unit area, regardless of the partitioning (ρ_s,ρ_b) of charges between the surface (ρ_s) and the brush (ρ_b). With increasing ρ the normal component of the electrostatic force repelling the chains from the surface increases and the chains first get oriented and then additionally extended in the direction perpendicular to the surface. This extension levels off (i.e., tends to a finite limit $\sim Nm^{-1/2}$) at large ρ, because of the strong screening by counterions which reside inside the grafted polyelectrolyte layer when the screening is sufficiently strong. The universal dimensionless scaling parameter $\lambda=\Lambda/H_0$ is found to determine the crossover between weak and strong screening regimes. Moreover, the average extension of chains in the limiting cases of single chain grafted to a charged surface and in case of the polyelectrolyte brush grafted to a neutral surface appear to be functions of a single parameter λ.

This universality breaks down, however, for the detailed conformational structure (density profiles, free-ends distribution, electrostatic field) in the brush, because these properties are very sensitive to the ratio $\beta=\rho_b/\rho$. With decreasing β (i.e., charging up the surface and simultaneously decreasing the grafting density) the average extension of chains in the z direction increases. The maximum in the monomer density profiles gets progressively displaced from the vicinity of the surface (for $\beta\cong 1$) to the peripheral region of the brush (for $\beta\ll 1$). The effect on the free ends is more pronounced: the edge maximum of the distribution becomes narrower and higher, while proximal to the surface region a dead zone (without ends) appears. In the intermediate range of β the free-end distribution becomes bimodal. This reflects the changing character of the fluctuations of the chain extension: from abnormally large ''quasicritical'' [39] fluctuation in the brush regime (large β) to the usual Gaussian fluctuations in the mushroom regime (small β).

ACKNOWLEDGMENTS

This research has been partially supported by the Dutch-Russian NWO project ''Polyelectrolytes in Complex Fluids,'' the Russian Fund for Fundamental Research (Grant No. 99-03-33319), and the National Science Foundation (No. DMR-9973300).

[1] P. A. Pincus, Macromolecules **24**, 2912 (1991).
[2] O. V. Borisov, T. M. Birshtein, and E. B. Zhulina, J. Phys. II **1**, 521 (1991).
[3] R. Ross and P. A. Pincus, Macromolecules **25**, 1503 (1992).
[4] E. B. Zhulina, O. V. Borisov, and T. M. Birshtein, J. Phys. II **2**, 63 (1992).
[5] O. V. Borisov, E. B. Zhulina, and T. M. Birshtein, Macromolecules **27**, 4795 (1994).
[6] J. Wittmer and J. F. Joanny, Macromolecules **26**, 2691 (1993).
[7] S. J. Miklavic and S. Marcelja, J. Phys. Chem. **92**, 6718 (1988).
[8] S. Misra, S. Varanasi, and P. P. Varanasi, Macromolecules **22**, 4173 (1989).
[9] S. Misra and S. Varanasi, J. Chem. Phys. **95**, 2183 (1991).
[10] S. Misra, W. L. Mattice, and D. H. Napper, Macromolecules **27**, 7090 (1994).
[11] R. Israels, F. A. M. Leermakers, G. J. Fleer, and E. B. Zhulina, Macromolecules **27**, 3249 (1994).
[12] R. Israels, F. A. M. Leermakers, and G. J. Fleer, Macromolecules, **27**, 3087 (1994).
[13] Yu. V. Lyatskaya, F. A. M. Leermakers, G. J. Fleer, E. B. Zhulina, and T. M. Birshtein, Macromolecules **28**, 3562 (1995).
[14] F. Goeler and M. Muthukumar, Macromolecules **28**, 6608 (1995).
[15] O. V. Borisov and E. B. Zhulina, J. Phys. II **7**, 449 (1997).
[16] E. B. Zhulina and O. V. Borisov, J. Chem. Phys. **107**, 5952 (1997).
[17] Y. Mir, P. Auroy, and L. Auvray, Phys. Rev. Lett. **75**, 2863 (1995).
[18] P. Guenoun, A. Schlachli, D. Sentenac, J. W. Mays, and J. J. Benattar, Phys. Rev. Lett. **74**, 3628 (1995).
[19] H. Watanabe, S. S. Patel, J. F. Argillier, E. E. Parsonage, J. Mays, N. Dan-Brandon, and M. Tirrell, Mater. Res. Soc. Symp. Proc. **249**, 255 (1992).
[20] M. Tirrell, in *Solvents and Self-Organization of Polymers*, NATO ASI Series E: Applied Sciences—327, 281 (Kluwer Academic, Dodrecht, 1996).
[21] P. Schorr, R. Toomey, M. Tirrell, D. Cook, and J. W. Mays, Proceedings of Yamada Conference L ''Polyelectrolytes,'' edited by I. Noda and E. Kokofuta, Japan, 393, 1999.
[22] D. H. Napper, Polymeric Stabilization of Colloidal Dispersions (Academic, London, 1985).
[23] C. G. de Kruif, Int. Dairy J. **9**, 183 (1999).
[24] E. B. Zhulina and O. V. Borisov, Macromolecules **31**, 7413 (1998).
[25] E. B. Zhulina, O. V. Borisov, J. van Male, and F. A. M. Leermakers, Langmuir (unpublished).
[26] O. V. Borisov, T. M. Birshtein, and E. B. Zhulina, J. Phys. II **4**, 913 (1994).
[27] J. N. Israelachvili, *Intermolecular and Surface Forces* (Academic, London, 1985).
[28] P. Pincus, Macromolecules **10**, 210 (1977).
[29] P. G. de Gennes, P. Pincus, R. M. Velasco, and F. Brochard, J. Phys. (France) **37**, 1461 (1976).
[30] A. R. Khokhlov and K. A. Khachaturian, Polymer **23**, 1742 (1982).
[31] A. N. Semenov, Sov. Phys. JETP **61**, 733 (1985).
[32] Instead of minimization of the free energy, Eq. (10) with respect to R_z, we can use the condition $E(z=R_z)=0$ of vanishing of local tension in the chain at the free end.
[33] A. M. Skvortsov, I. V. Pavlushkov, A. A. Gorbunov, E. B. Zhulina, O. V. Borisov, and V. A. Pryamitsyn, Polym. Sci. U.S.S.R. **30**, 1706 (1988).
[34] E. B. Zhulina, O. V. Borisov, V. A. Pryamitsyn, and T. M. Birshtein, Macromolecules **24**, 140 (1991).
[35] E. B. Zhulina, O. V. Borisov, and V. A. Pryamitsyn, J. Colloid Interface Sci. **137**, 495 (1991).
[36] G. J. Fleer, M. A. Cohen, J. M. H. M. Scheutjens, T. Cosgrove, and B. Vincent, *Polymers at Interfaces* (Chapman & Hall, London, 1993).
[37] O. A. Evers, J. M. H. M. Scheutjens, and G. J. Fleer, Macromolecules **23**, 5221 (1990).
[38] From a mathematical point of view the jump in the monomer density profile and divergency in the free-end distribution are essentially related to each other via Eq. (30).
[39] L. I. Klushin and A. M. Skvortsov, Macromolecules **24**, 1549 (1991).